Turbulence modulation and drag reduction by spherical particles

L. H. Zhao,[1] H. I. Andersson,[1] and J. J. J. Gillissen[2]
[1]*Department of Energy and Process Engineering, Norwegian University of Science and Technology, 7491 Trondheim, Norway*
[2]*Department of Multi-Scale Physics, TU Delft, 2628 BW Delft, The Netherlands*

(Received 13 May 2010; accepted 21 July 2010; published online 16 August 2010)

This letter reports on the pronounced turbulence modulations and the accompanying drag reduction observed in a two-way coupled simulation of particle-laden channel flow. The present results support the view that drag reduction can be achieved not only by means of polymeric or fiber additives but also with spherical particles. © *2010 American Institute of Physics*.
[doi:10.1063/1.3478308]

The inevitable pressure loss associated with transport of fluids in pipelines determines the pumping requirements. The pressure loss arises in order to overcome the skin-friction drag. Several investigations of turbulent drag reduction have thus been motivated by the economical benefits of pressure-loss reduction. Drag reduction can be achieved in many different ways, for instance, by means of additives suspended into an otherwise Newtonian fluid (see, e.g., the reviews by Lumley[1] and Gyr and Bewersdorff[2]). A notable example is the substantial drag reduction observed when flexible polymers are dissolved in the carrier fluid as reported in Refs. 3 and 4 (see also the recent reviews[5,6]). However, the findings with respect to drag reduction are not as clear-cut for additives other than polymers and chemicals. Pressure drop measurements reported from a variety of solid-fluid systems were scrutinized by Radin *et al.*[7] While drag reduction was obtained with fibrous additives (e.g., nylon or cotton), no drag reduction was reported for nonfibrous additives irrespective of the shape of the solid (spherical, platelet, or needle-shaped). More recently, drag reduction has been reported from computer experiments by Paschkewitz *et al.*[8] and Gillissen *et al.*[9] also for rigid fibers.

Suspensions of *spherical* particles in turbulent pipe and channel flows have been extensively studied during the years with the view to better understand the particle transport, dispersion, and segregation in wall-turbulence and also the influence of the presence of the solid spheres on the turbulence of the carrier fluid. The current understanding of the complex behavior of inertial spherical particles in turbulent wall flows was summarized in a keynote lecture by Soldati.[10] The survey of experimental studies and two-way coupled computer simulations by Balachandar and Eaton[11] furthermore addressed the turbulence modulation observed in the presence of inertial particles. In dilute suspensions where particle collisions are of negligible importance, the fluid turbulence may be affected by an enhanced dissipation due to the particles, kinetic energy transfer between the fluid and the particles, and wakes formed in the lee of the solid particles. The relative importance of these mechanisms depends on the particle Reynolds number, the particle-to-fluid density ratio, and the particle-to-turbulence length-scale ratio. By adopting the turbulence intensity as a measure of the turbulence activity, Gore and Crowe[12] showed that a particle diameter of 1/10 the size of the most energetic eddies represents a demarcation between increase and decrease of the carrier-phase turbulence such that smaller particles tended to attenuate the turbulence.

In this letter, turbulence attenuation in a dilute suspension of spherical particles is further explored. A reduced turbulence activity in the presence of tiny spheres has been observed in several laboratory experiments[13,14] and computer simulations.[15–17] In most cases, the attenuation of the turbulence is associated with a substantial reduction of the velocity fluctuations perpendicular to the mean flow, whereas the streamwise turbulence intensity might be enhanced. These alterations of the fluctuating velocity field reflect a higher degree of asymmetry. The same trends have been reported in conjunction with drag reduction, for instance, in dilute polymer solutions.[3,4] Evidence of drag reduction achieved by means of spherical particles is, however, almost nonexisting. Rashidi *et al.*[18] showed that the presence of small particles reduced the number of wall ejections, turbulence intensity, and also the skin friction. A modest pressure-loss reduction was also reported for the smallest particle case considered in the pipe-flow experiments by Kartushinsky *et al.*[19] More recent pressure-drop measurements by Bari and Yunus[20] showed substantial drag reduction for suspensions of either alumina or sand particles in kerosene over a fairly wide range of turbulent Reynolds numbers. Drag reduction was also found in the computer experiments by Li *et al.*,[16] but their mesh was too coarse to assure accurate results. The more reliable simulations by Dritselis and Vlachos[21] suggested a modest drag reduction, although not commented by the authors. For a given bulk velocity, the wall-friction was reduced by 4% in the particle-laden flow. On the basis of the above observations, it may be conjectured that significant drag reduction can be achieved also by means of small spherical particles, provided that the particle size, density, and loading are properly selected.

We consider the fully developed turbulent flow in a plane channel. The motion of the incompressible Newtonian fluid is governed by the continuity and momentum conservation equations

 © 2010 American Institute of Physics

Downloaded 25 Aug 2010 to 131.180.130.114. Redistribution subject to AIP license or copyright; see http://pof.aip.org/about/rights_and_permissions

$$\nabla \cdot \vec{u} = 0, \quad \rho\left[\frac{\partial \vec{u}}{\partial t} + (\vec{u}\cdot\nabla)\vec{u}\right] = -\nabla p + \mu\nabla^2\vec{u} + \vec{F}_p. \quad (1)$$

Here, $\vec{u}$ and p are the instantaneous fluid velocity vector and pressure, respectively, whereas $\vec{F}_p$ denotes the force per unit volume from the particles. ρ and μ are the density and the dynamic viscosity of the Newtonian carrier fluid.

The translational motion of individual spherical particles is governed by Newton's second law. Only the Stokes drag is considered in present work, while other forces, such as lift and virtual-mass forces, are neglected. The particle Reynolds number $\mathrm{Re}_p = 2a|\vec{u}-\vec{v}|\rho/\mu$, based on the particle diameter $2a$ and the slip velocity between the fluid and particle, should be smaller than unity to satisfy the assumption of Stokes flow in the particle vicinity. The size of the particles is smaller than smallest eddies in the flow such that the force $\vec{f}_i(\vec{x}_p)$ on particle number i can be treated as a point force

$$\vec{f}_i(\vec{x}_p) = 6\pi\mu a[\vec{u}(\vec{x}_p,t) - \vec{v}]. \quad (2)$$

Here, $\vec{v}$ is the translational velocity of the particle and $\vec{u}$ is the fluid velocity evaluated at the particle location $\vec{x}_p$. The motion of a particle and its trajectory are obtained from

$$\frac{d\vec{v}}{dt} = \frac{1}{\tau}[\vec{u}(\vec{x}_p,t) - \vec{v}], \quad \frac{d\vec{x}_p}{dt} = \vec{v}. \quad (3)$$

The particle response time τ can be expressed as

$$\tau = \frac{2\rho D a^2}{9\mu}, \quad (4)$$

under the Stokes flow approximation where $D = \rho_p/\rho$ is the ratio between the particle and fluid densities. The particles collide elastically with the walls. If a particle hits a wall, it bounces back into the flow with the only change that the wall-normal velocity component switches sign.

The Lagrangian particle equations (3) are integrated forward in time along with the Eulerian equation (1) for the fluid motion in a two-way coupled simulation. Each and every particle acts back onto the fluid with a point force $-\vec{f}_i(\vec{x}_p)$, in accordance with Newton's third law. The feedback from the n_p particles within a given grid cell volume V_{cell} adds up

$$\vec{F}_p = -\frac{1}{V_{\mathrm{cell}}}\sum_{i=1}^{n_p}\vec{f}_i(\vec{x}_p). \quad (5)$$

This is the force per unit volume in the particle-laden Navier–Stokes equation (1). This point-force approach to two-way coupled simulations is essentially the same as that introduced by Squires and Eaton[22] for isotropic turbulence and subsequently adopted for wall-bounded turbulence.[16,21,23]

The governing equations for the fluid and particle motions can be normalized by the skin-friction velocity u_* and the channel height h. This gives the following set of partial and ordinary differential equations:

$$\nabla \cdot \vec{u} = 0, \quad \frac{\partial \vec{u}}{\partial t} + (\vec{u}\cdot\nabla)\vec{u} = +2\vec{e}_x - \nabla p + \mathrm{Re}^{-1}\ \nabla^2\vec{u} + \vec{\tilde{F}}_p, \quad (6)$$

$$\frac{d\vec{v}}{dt} = \frac{1}{\tilde{\tau}}[\vec{u}(\vec{x}_p,t) - \vec{v}], \quad \frac{d\vec{x}_p}{dt} = \vec{v}. \quad (7)$$

All dependent and independent variables are now dimensionless quantities, although we stick to the same notation as for the dimensional variables. The first term to the right of Eq. (6) is the imposed mean pressure gradient, which drives the flow in the positive x-direction. The normalized particle relaxation time $\tilde{\tau}$ in Eq. (7) is

$$\tilde{\tau} = \frac{\tau}{h/u_*} = \frac{2}{9}D(\tilde{a})^2\mathrm{Re}, \quad (8)$$

where $\tilde{a} = a/h$ and $\mathrm{Re} = \rho u_* h/\mu$ is the wall-friction Reynolds number. The particles in a given grid cell act on the fluid flow by means of the force

$$\vec{\tilde{F}}_p = -6\pi\ \mathrm{Re}^{-1}\ \tilde{a}\frac{1}{\tilde{V}_{\mathrm{cell}}}\sum_{i=1}^{n_p}[\vec{u}(\vec{x}_p,t) - \vec{v}]. \quad (9)$$

Here, $\tilde{V}_{\mathrm{cell}}$ is the dimensionless volume of the grid cell.

In *one-way coupled* simulations, the influence of the particles on the flow field through $\vec{\tilde{F}}_p$ is either ignored or negligibly small and the flow field is determined only by the friction Reynolds number, Re. The particle dynamics are fully determined when also $\tilde{\tau}$ is given. Thus, for a given Re, a short particle relaxation time, i.e., a fast particle response, corresponds to either light or small particles (low values of either D or $\tilde{a}$) according to Eq. (8). In *two-way coupled* simulations, on the other hand, the feedback from the particles on the fluid motion is given by Eq. (9), which shows that the magnitude of the feedback is determined by the particle size $\tilde{a}$ but is independent of the relative particle density D. Thus, $\tilde{a}$ and D play different roles in two-way coupled simulations and cannot be combined into a single parameter $D(\tilde{a})^2$ as in one-way coupled simulations.

The turbulent channel flow was driven by the prescribed pressure gradient corresponding to a friction Reynolds number $\mathrm{Re} = 360$. The sizes of the computational domain were $6h$ and $3h$ in the streamwise x-direction and the spanwise y-direction, respectively. Periodic boundary conditions were imposed in these homogeneous directions and no-slip and impermeability were enforced at the solid walls at $z = 0$ and $z = h$. The computational mesh consisted of 128^3 grid points. The direct numerical simulations (DNSs) were performed with the same Navier–Stokes solver as used by Gillissen *et al.*[24] and Mortensen *et al.*[25] After the turbulent flow field first had evolved into a statistically steady state, 4×10^6 spherical particles were randomly released into the flow field. The particle radius $\tilde{a}$ was 0.001 and the density ratio $D = 1042$. This corresponds to $a^+ = 0.36$ and $\tau^+ = 30$ in terms of the viscous scales ν/u_* and ν/u_*^2 for length and time, respectively. The particle characteristics were thus the same as those in the one-way coupled simulations (case C) by Mortensen *et al.*[25]

The particle-laden channel flow was assumed to be sufficiently dilute so that particle-particle collisions were of negligible importance, i.e., the flow was in the two-way coupling regime according to the updated classification map due

Downloaded 25 Aug 2010 to 131.180.130.114. Redistribution subject to AIP license or copyright; see http://pof.aip.org/about/rights_and_permissions

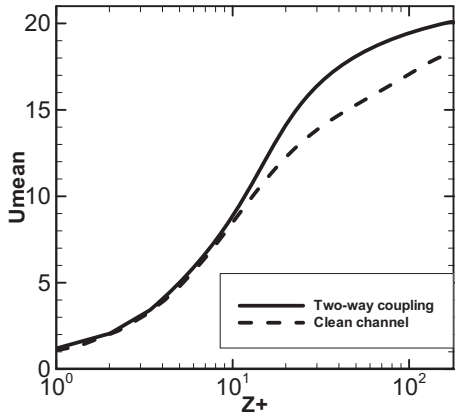

FIG. 1. Mean fluid velocity profile $U^+(z^+)$ for the particle-laden channel flow (solid line) and for the unladen flow (broken line).

to Elghobashi.[26] For a given grid cell, the force $\vec{F}_p$ from the particles on the fluid is a sum of point forces according to Eq. (9). In practice, a point force, which originated from the hydrodynamic force (2) on an individual particle at $\vec{x}_p$, was considered as a body force $-\vec{f}_i(\vec{x}_p)/V_{\text{cell}}$ that acted in the cell center. In accordance with the quasistaggered grid system, however, the wall-normal force component was assigned to the nearest wall-parallel cell face rather than to the cell center. No smoothing of the forces from the particles onto the fluid was required.

The same time step $\Delta t=0.0001h/u_*$ as in the DNS was used for the integration of the particle equations of motion (7). This time step corresponds to $\Delta t^+=0.036$ measured in viscous time units. The particles were released into an already statistically steady unladen channel flow. The simulation of the particle-laden flow was first run for $20h/u_*$ $(7200\nu/u_*^2)$. During this time span, the particles accumulated in the near-wall region. The bulk flow was monitored and seemed to reach an almost steady state during this period of time. The simulation was thereafter continued for another $5h/u_*$, during which fluid and particle statistics were gathered.

The results of the two-way coupled simulation will be compared with results from a clean or unladen channel simulation, i.e., with $\vec{F}_p=0$ in the particle-laden Navier–Stokes equation (1). The same computational domain and the same grid were used in both simulations and the wall-friction Reynolds number was the same, i.e., Re=360. The mean fluid velocity in Fig. 1 is substantially increased compared with that in the clean channel. Since Re and thus u_* are the same in both cases, the enhanced mean velocity is equivalent with drag reduction. Here, the bulk flow rate is 14% higher than for the particle-free flow driven by the same pressure gradient. In view of this finding, it is not surprising to observe the dramatic alterations of the turbulence field in Fig. 2. The streamwise turbulence intensity shown in Fig. 2(a) is enhanced and the peak position is shifted somewhat further away from the wall than in the unladen channel. On the contrary, the velocity fluctuations perpendicular to the mean-flow direction are reduced considerably, as seen in Figs. 2(b) and 2(c). The increased anisotropy of the fluid turbulence due to the solid particles can either be due to different time

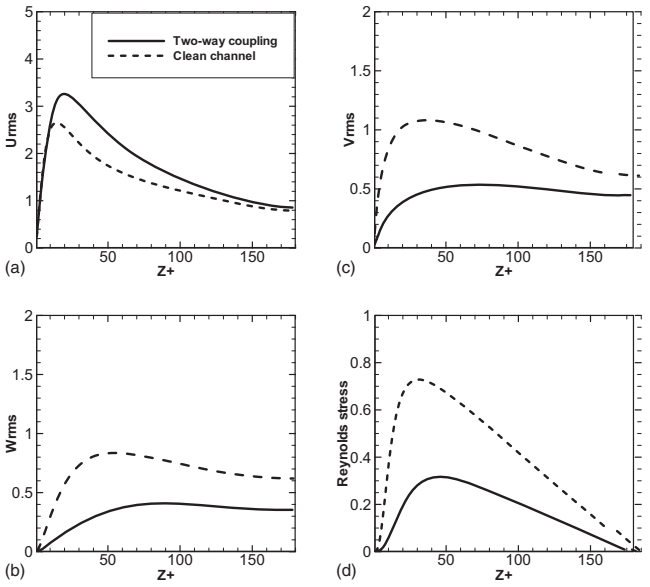

FIG. 2. Turbulence intensities and Reynolds shear stress for the particle-laden channel flow (solid lines) and for the unladen flow (broken lines). (a) Streamwise intensity u_{rms}; (b) cross-stream intensity v_{rms}; (c) wall-normal intensity w_{rms}; and (d) Reynolds shear stress $-\overline{uw}$.

scales (or frequencies) of the different components of the instantaneous velocity vector or a hampered intercomponential energy transfer due to pressure-strain interactions. The pronounced reduction of the Reynolds shear stress $-\overline{uw}$ in Fig. 2(d) is partly due to the reduced wall-normal fluctuations and also a consequence of a decorrelation between the streamwise and wall-normal velocity components.

The trends exhibited by the fluid statistics in Figs. 1 and 2 are the same as when drag reduction is achieved by means of polymeric additives, e.g., Ptasinski *et al.*,[3] Dubief *et al.*,[4] and Graham.[5] Spherical particles have occasionally given rise to the same qualitative effect on the turbulence field, but

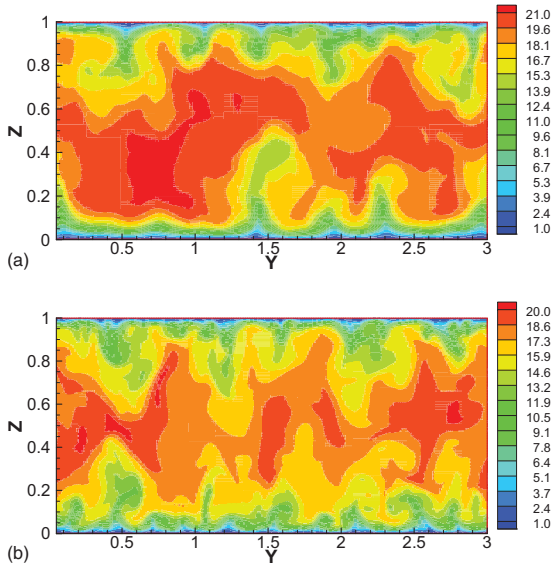

FIG. 3. (Color online) Instantaneous contours of the streamwise velocity component in a cross-sectional (y,z)-plane. Not to scale. (a) Particle-laden flow and (b) unladen flow.

Downloaded 25 Aug 2010 to 131.180.130.114. Redistribution subject to AIP license or copyright; see http://pof.aip.org/about/rights_and_permissions

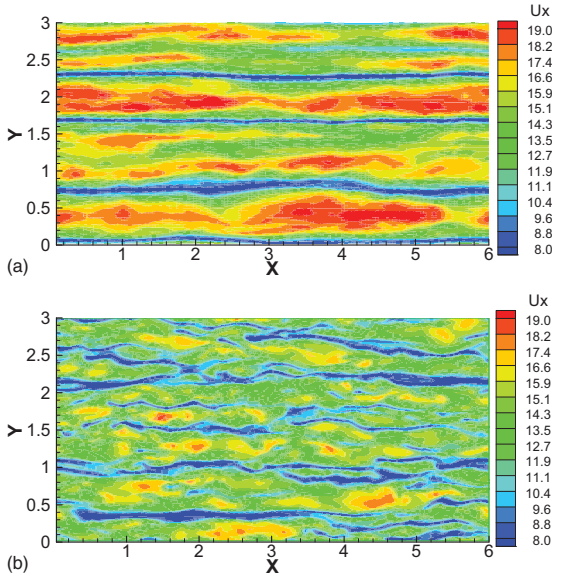

FIG. 4. (Color online) Instantaneous contours of the streamwise velocity component in a (x,y)-plane at $z^+=20$. Not to scale. (a) Particle-laden flow and (b) unladen flow.

without any reported drag reduction except in the under-resolved DNS-study of Li *et al.*[16]

Contours of the instantaneous streamwise fluid velocity are presented in Figs. 3 and 4. The smaller scales, which appear as distortions of the large-eddy contours, have been damped in the particle-laden flow, both in the cross-sectional plane in Fig. 3 and in the wall-parallel plane in Fig. 4. The streamwise coherence of the near-wall flow structures is considerably increased in the presence of particles. The alternating high- and low-velocity bands in Fig. 4(a) appear wider and more regular than in the unladen flow. This is a typical feature of drag-reduced flows independent of the actual cause of drag reduction, for instance, polymer-induced drag reduction (see, e.g., Ref. 6). The close resemblance of the present flow modulations and the turbulence modulations associated with fiber- and polymer-induced drag reduction makes us believe that also the spherical particles interrupt the turbulence generating cycle by a reduction of the strength and number of quasistreamwise vortices, which, in turn, leads to stabilization and widening of the near-wall streaks.

Pronounced turbulence modulations have been observed in the present two-way coupled simulation of turbulent channel flow laden with spherical particles. The enhancement of the turbulence anisotropy and the attenuation of the Reynolds shear stress are typical findings when drag reduction is achieved by means of polymeric or fiber additives. It is therefore not unexpected that significant drag reduction is found also when the turbulence is modulated by tiny spherical particles. The present results support the recently measured pressure-loss reductions achieved by means of sand or alumina particles in a liquid circulation loop.[20]

This work has been supported by A/S Norske Shell through a research fellowship (Contract No. 4610020178/C08156) and by The Research Council of Norway (Programme for Supercomputing) through a grant of computing time.

[1] J. L. Lumley, "Drag reduction by additives," Annu. Rev. Fluid Mech. **1**, 367 (1969).
[2] A. Gyr and H. W. Bewersdorff, *Drag Reduction of Turbulent Flows by Additives* (Kluwer, Dordrecht, 1995).
[3] P. K. Ptasinski, B. J. Boersma, F. T. M. Nieuwstadt, M. A. Hulsen, B. H. A. A. van den Brule, and J. C. R. Hunt, "Turbulent channel flow near maximum drag reduction: Simulations, experiments and mechanisms," J. Fluid Mech. **490**, 251 (2003).
[4] Y. Dubief, C. M. White, V. E. Terrapon, E. S. G. Shaqfeh, P. Moin, and S. K. Lele, "On the coherent drag-reducing and turbulent-enhancing behaviour in wall flows," J. Fluid Mech. **514**, 271 (2004).
[5] M. D. Graham, "Drag reduction in turbulent flow of polymer solutions," *Rheology Reviews* (British Society of Rheology, Norwich, UK, 2004), pp. 143–170.
[6] C. M. White and G. Mungal, "Mechanics and prediction of turbulent drag reduction with polymer additives," Annu. Rev. Fluid Mech. **40**, 235 (2008).
[7] I. Radin, J. L. Zakin, and G. K. Patterson, "Drag reduction in solid-fluid systems," AIChE J. **21**, 358 (1975).
[8] J. S. Paschkewitz, Y. Dubief, C. D. Dimitropoulus, E. S. G. Shaqfeh, and P. Moin, "Numerical simulation of turbulent drag reduction using rigid fibres," J. Fluid Mech. **518**, 281 (2004).
[9] J. J. J. Gillissen, B. J. Boersma, P. H. Mortensen, and H. I. Andersson, "Fibre-induced drag reduction," J. Fluid Mech. **602**, 209 (2008).
[10] A. Soldati, "Particles turbulence interactions in boundary layers," Z. Angew. Math. Mech. **85**, 683 (2005).
[11] S. Balachandar and J. K. Eaton, "Turbulent dispersed multiphase flow," Annu. Rev. Fluid Mech. **42**, 111 (2010).
[12] R. A. Gore and C. T. Crowe, "Modulation of turbulence by a dispersed phase," Trans. ASME J. Fluids Eng. **113**, 304 (1991).
[13] J. D. Kulick, J. R. Fessler, and J. K. Eaton, "Particle response and turbulence modification in fully developed channel flow," J. Fluid Mech. **277**, 109 (1994).
[14] S. Geiss, A. Dreizler, Z. Stojanovic, M. Chrigui, A. Sadiki, and J. Janicka, "Investigation of turbulence modification in a non-reactive two-phase flow," Exp. Fluids **36**, 344 (2004).
[15] Y. Pan and S. Banerjee, "Numerical simulation of particle interactions with wall turbulence," Phys. Fluids **8**, 2733 (1996).
[16] Y. Li, J. B. McLaughlin, K. Kontomaris, and L. Portela, "Numerical simulation of particle-laden turbulent channel flow," Phys. Fluids **13**, 2957 (2001).
[17] J. K. Eaton, "Two-way coupled turbulence simulations of gas-particle flows using point-particle tracking," Int. J. Multiphase Flow **35**, 792 (2009).
[18] M. Rashidi, G. Hetsroni, and S. Banerjee, "Particle-turbulence interaction in a boundary layer," Int. J. Multiphase Flow **16**, 935 (1990).
[19] A. Kartushinsky, A. Mulgi, S. Tisler, and E. E. Michaelides, "An experimental study of the effect of particles on the shear stress in particulate turbulent pipe flow," Proc. Estonian Acad. Sci. Eng. **11**, 161 (2005).
[20] H. A. A. Bari and R. B. M. Yunus, "Drag reduction improvement in two phase flow system using traces of SLES surfactant," Asian J. Ind. Eng. **1**, 1 (2009).
[21] C. D. Dritselis and N. S. Vlachos, "Numerical study of educed coherent structures in the near-wall region of a particle-laden channel flow," Phys. Fluids **20**, 055103 (2008).
[22] K. D. Squires and J. K. Eaton, "Particle response and turbulence modification in isotropic turbulence," Phys. Fluids A **2**, 1191 (1990).
[23] M. Picciotto, A. Giusti, C. Marchioli, and A. Soldati, "Turbulence modulation by micro-particles in boundary layers," *IUTAM Symposium on Computational Approaches to Multiphase Flow*, edited by S. Balachandar and A. Prosperetti (Springer, Dordrecht, 2006), pp. 53–62.
[24] J. J. J. Gillissen, B. J. Boersma, P. H. Mortensen, and H. I. Andersson, "On the performance of the moment approximation for the numerical computation of fibre stress in turbulent channel flow," Phys. Fluids **19**, 035102 (2007).
[25] P. H. Mortensen, H. I. Andersson, J. J. J. Gillissen, and B. J. Boersma, "Particle spin in a turbulent shear flow," Phys. Fluids **19**, 078109 (2007).
[26] S. Elghobashi, "An updated classification map of particle-laden turbulent flows," *IUTAM Symposium on Computational Approaches to Multiphase Flow*, edited by S. Balachandar and A. Prosperetti (Springer, Dordrecht, 2006), pp. 3–10.

Downloaded 25 Aug 2010 to 131.180.130.114. Redistribution subject to AIP license or copyright; see http://pof.aip.org/about/rights_and_permissions